**Proceedings of the Canadian Society for Mechanical Engineering International Congress 2022**
**CSME Congress 2022**
**June 5-8, 2022, Edmonton, AB, Canada**

# Co-flow Droplet Generator with a Deformable Wall

Sajad Yazdanparast, Pouya Rezai, Alidad Amirfazli*
Department of Mechanical Engineering, York University, Toronto, Canada
*alidad2@yorku.ca

***Abstract***— We propose a simple microfluidic droplet generator for controlling the droplet size over a wide range. A planar co-flow device was developed with controllable c-phase channel width using a deformable wall structure. The design was benefited from the increased shear force due to the channel width decrease and controlled droplet size. The range of droplets sizes was boosted in the proposed device by 111% compared to the reported devices in the literature. Two distinct regimes were observed: dripping (at high and medium channel widths) and plug regimes (at low channel widths). Droplets were monodispersed in both regimes. Also, the effect of channel width on the droplet size at constant c-phase velocities and flow rates was investigated. The rate of change in droplet diameter was more at a constant flow rate compared to constant c-phase velocity.

***Keywords- Droplet microfluidics; Co-flow droplet generation method; Controlling droplet size; flexible walls***

## I. INTRODUCTION

Microfluidic droplet generation has received considerable attention in the last two decades. Droplet microfluidics provides a uniform condition for (micro)droplets, leading to monodisperse droplets. Monodispersity is essential for various applications of microdroplets, i.e., drug delivery [1]–[3], molecular synthesis [4] , diagnostics [5], [6], chemical reactions [7], imaging [8]–[10], and food processing and production [11], [12].

The dispersed phase (d-phase) droplets are generated in an immiscible fluid called the continuous phase (c-phase). D-phase and c-phase channels are parallel in the co-flow method. The co-flow method has three distinct regimes, i.e., dripping, narrow jetting, and wide jetting [13]. Dripping regime occurs at low c-phase Capillary number ($Ca_c < 0.1$) and low d-phase Weber number ($We_d < 0.1$) [13]. Droplets are pinched off at the capillary tip in the dripping regime [14], [15]. The droplets were generated in the dripping regime in the current work to have monodispersed droplets [14], [16].

C-phase flow rate ($Q_c$) conventionally is used to control droplet size [14], [15], [17]. But relying just on the c-phase flow rate to change the droplet size in a wide range is not sufficient. If the flow rate exceeds a certain value, the viscous force becomes dominant, leading to the narrow jet regime. C-phase channel size ($D_c$) can be used to control droplet size through its effect on the drag force [18].

Previous works switched devices to alter the c-phase channel size [17]. In this paper, the c-phase channel width was tuned on-demand in a single device by squeezing the device's walls. We benefited from the enhanced wall effect due to the channel width decrease and changed droplets sizes over a wide range.

## II. EXPERIMENTAL PROCEDURES

### A. Materials

PDMS (Sylgard 184 kit, Dow Corning, USA) was prepared with a 10:1 ratio of monomer to curing agent. The flexible silicon tubing was purchased from Antylia Scientific. Pulled glass capillary (OD: 1.0 mm, 1B100–4, World Precision Instruments, USA) was utilized as the dispensing nozzle in the PDMS channel. Deionized (DI) water and silicone oil (Silicone oil, Sigma-Aldrich co., Germany) were used as d-phase and c-phase, respectively. Table I shows the physical properties of d-phase and c-phase.

TABLE I. PHYSICAL PROPERTIES OF D-PHASE AND C-PHASE

| ***Phase*** | ***Material*** | ***Density ($Kg/m^3$)*** | ***Viscosity (cSt)*** | ***Interfacial tension (mN/m)*** |
|---|---|---|---|---|
| *D-phase* | *Di water* | *998* | *1.004* | *35.26* [19] |
| *C-phase* | *Silicone oil* | *960* | *50* | |

### B. Design and Fabrication

The co-flow droplet generator with flexible walls, shown in Figure 1, consisted of a PDMS segment with one inlet and one outlet, a glass capillary, two moving blocks, two micro-positioners, and a fixture. Two micro-positioners precisely pushed the moving blocks to squeeze the channel. The channel had two sections (see Figure 3), a wide section (with a rectangular cross-section of 2 × 1.1 mm) at first, and then it gradually merged to a narrow section (with a rectangular cross-

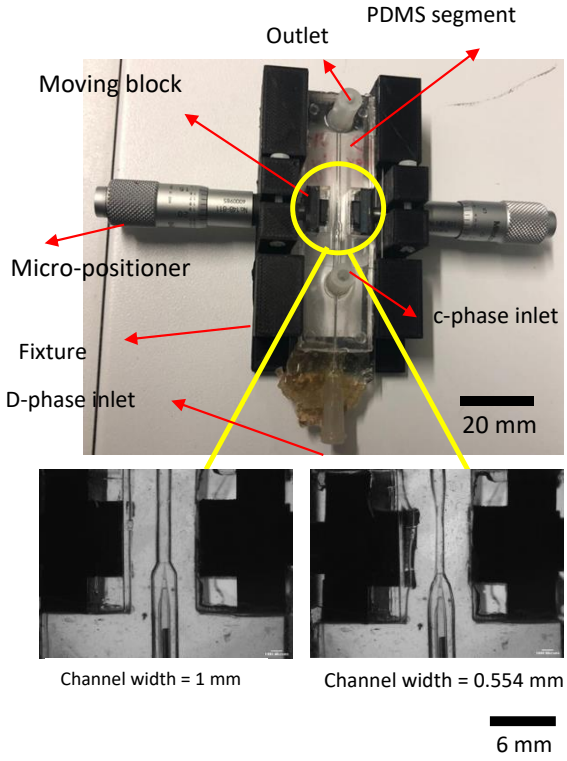


Figure 1. The developed device consisted of a PDMS segment, a glass capillary for d-phase inlet, two moving blocks for squeezing the channel, a fixture, and two micro-positioners for pushing the moving blocks (top). Channel width was decreased from 1 mm to 0.554 mm by moving blocks (bottom).

section of 1 × 1 mm). The capillary tip was fixed at the beginning of the narrow section. The channel width can be changed from 1 to 0.3 mm.

The PDMS segment was fabricated using the soft lithography technique with molds being 3D printed using Objet 260 Connex (Stratasys Ltd, USA). The base monomer and curing agent mixture were degassed in a vacuum chamber for 40 min. The tubes for the inlet and the outlet were connected to the top layer mold, and the degasified PDMS was poured on the molds and heated at 85 ºC for 3 hours. The cured PDMS layers were carefully peeled off from the replication molds. After fixing the glass capillary at their predetermined position at the bottom layer, the bottom and top layers were bonded after placing them in a plasma cleaner (Harrick Plasma, PDC-001, USA). Then the top and bottom of the PDMS segment (except the squeezing area) were bonded to two glass slides using the same plasma bonding machine. The two moving blocks were placed at the predetermined position. The assembly of the PDMS segment, glass slides, and moving blocks was inserted into a fixture. To push moving blocks, two micro-positioners (MTT148-502, Mitutoyo Co., Japan) were attached to the fixture.

### *C. Experimental Setup and Droplet Size Measurement*

The experimental setup, presented in Figure 2, comprised a device, a high-speed camera (IL5, Fastec Imaging Corp., USA), a d-phase syringe pump (210 Legacy, KD Scientific, USA), a c-phase syringe pump (LEGATO 210, KD Scientific, USA), a data acquisition system, and a collecting container. Image processing was carried out using image analysis software (ImageJ, USA) to measure droplets sizes.

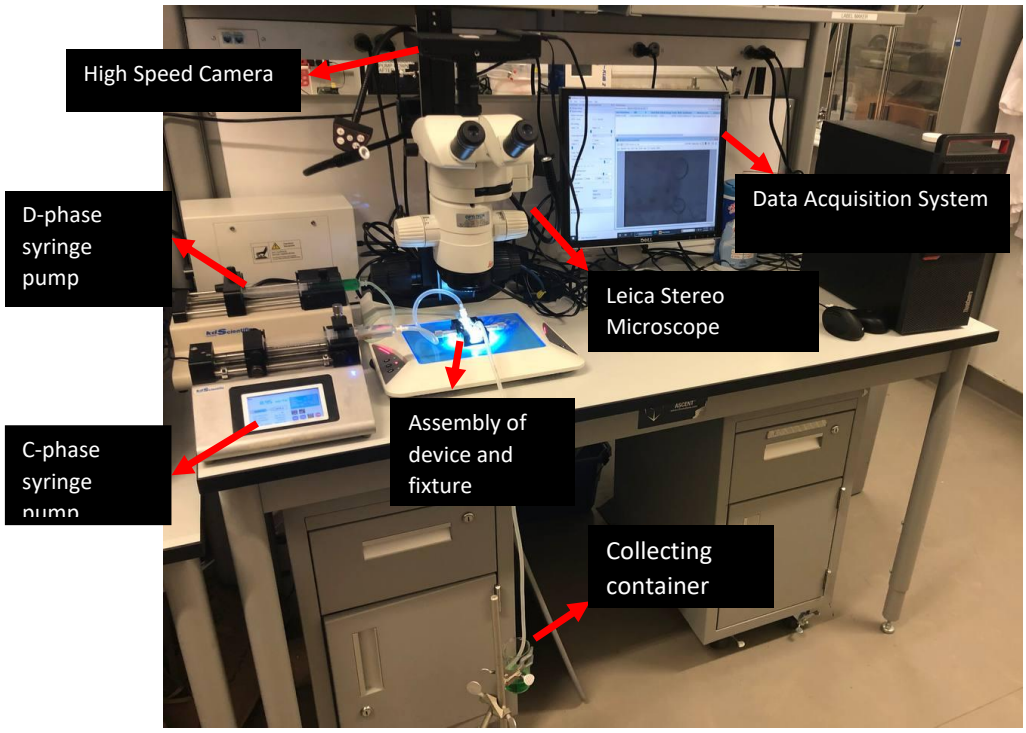


Figure 2. Experimental setup, consisted of the device, high-speed camera, microscope, data acquisition system, c-phase, and d-phase syringe pumps, and collecting reservoir

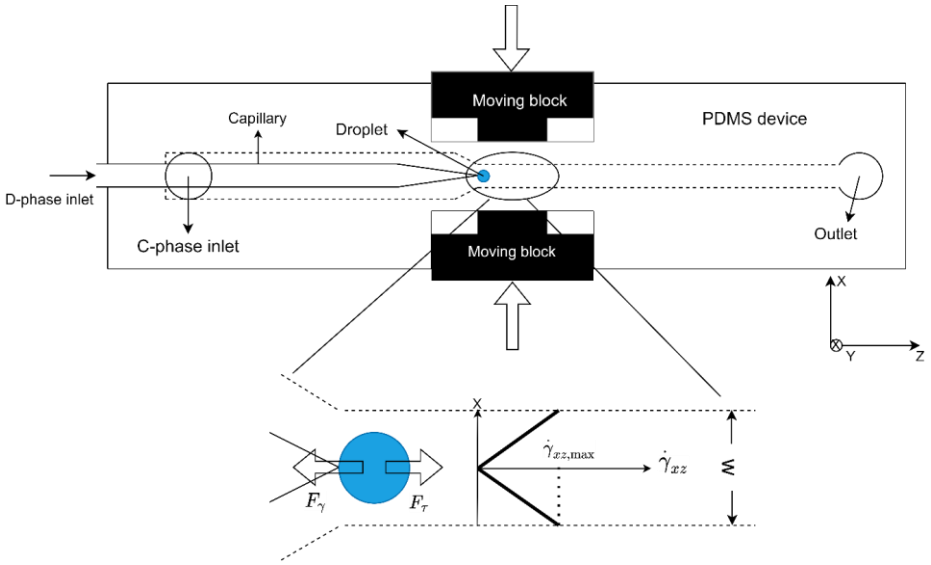


Figure 3. Experimental setup, consisted of the device, high-speed camera, microscope, data acquisition system, c-phase, and d-phase syringe pumps, and collecting reservoir

## III. WORKING PRINCIPLE

The working principle of the proposed device is based on viscous and interfacial tension forces being dominant as the system operated in the dripping regime (Figure 3). Any factor that affects the force balance can change droplet size. A decrease in the channel width leads to an increase in the viscous force by increasing the shear rate. The increased viscous force causes the droplet pinch-off to happen at a smaller droplet diameter.

## IV. RESULTS AND DISCUSSION

Two distinct regimes were observed in this study, the dripping regime (Figure 4 (a)) and the plug regime (Figure 4 (b)). The droplet grew enough to touch the lateral walls in the plug regime while the channel width was at its minimum level (0.3 mm). This was the main difference between the dripping and the plug regime. The important forces in the plug regime were similar to that in the dripping regime, which were interfacial tension and viscous forces. This was because the c-phase could bypass the plug easily due to the large gap between the plug and the top and bottom surfaces of the channel. Also, the polydispersity was low for both regimes. Figure 5 shows that the medians of polydispersities in the dripping and plug regimes were less than 2%.

Figure 6 shows the largest (913 µm), and smallest (175 µm) generated droplets. The developed device showed its advantage over the current designs in the literature as it generates droplets over a wide range. This is done, using tunable channel size along with changing c-phase flow rate made it possible to control droplet sizes over a range of 738 µm. This range was exceptionally wider (111%) compared to the reported device in

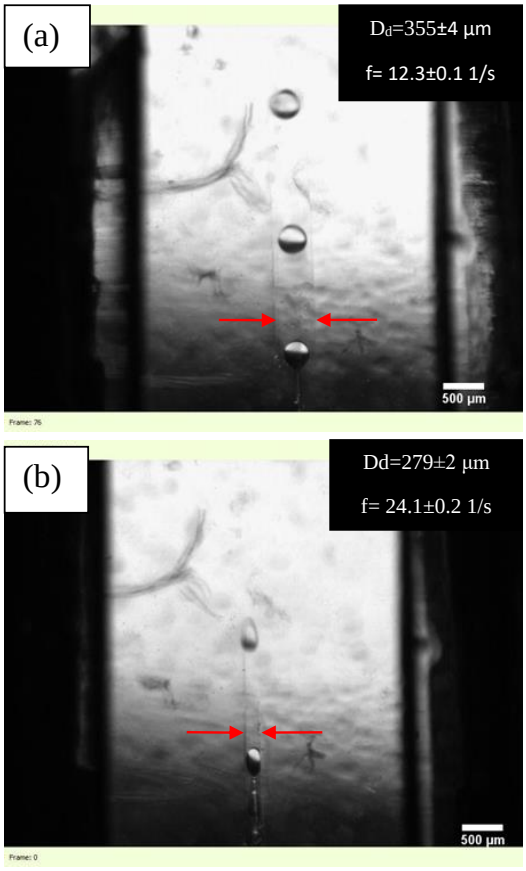


Figure 4. Various droplet generation regimes in the proposed device with (a) dripping regime at w=0.65mm and (b) plug regime at w=0.3mm. Cases of (a) and (b) both were under similar conditions in terms $u_c$ = 5 mm/s, $Q_d$ = 1 ml/hr, $Ca_c$ = 0.007, and $We_d$ = 0.0052. $D_d$ and f are droplet diameter and droplet generation frequency, respectively. Red arrows show the channel walls.

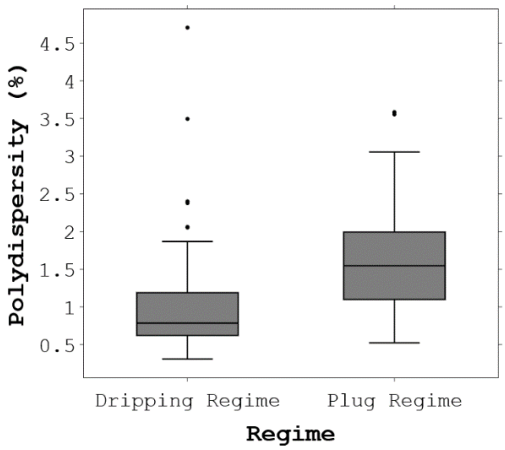


Figure 5. Box plot of polydispersity for the regimes observed in the current study. The medians of polydispersities in the dripping and plug regimes are less than 2%.

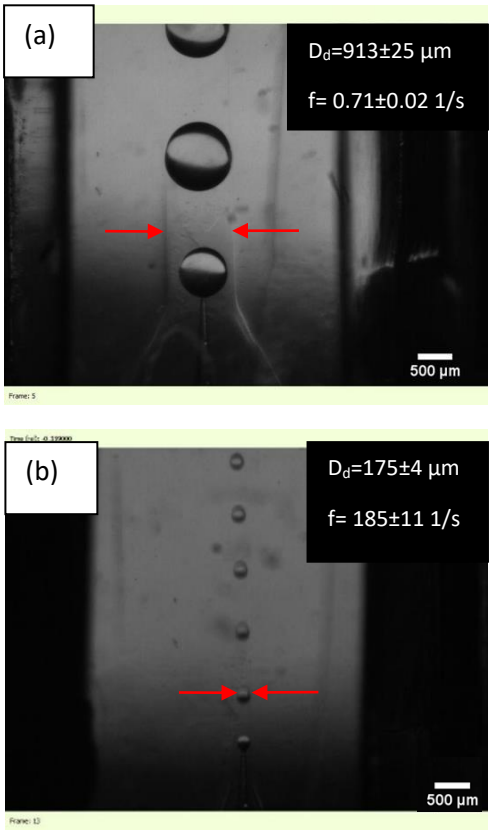


Figure 6. Maximum and minimum droplets sizes, $D_d$, generated in the current project. (a) Droplets with the size of 913 µm generated at w = 1 mm and $Q_c$ = 2 ml/hr. (b) Droplets with the size of 175 µm generated at w = 0.3 mm and $Q_c$ = 50 ml/hr. Red arrows show the channel walls.

which the widest range of droplets was generated (about 350 µm) [20].

Under two conditions, the channel was squeezed: constant c-phase velocity and constant c-phase flow rate. Figure 7 compares the effect of channel width on droplet size under these two conditions. Decrease of channel width at constant velocity led to the reduction of droplet diameter by increasing shear rate. Droplet diameter underwent a greater change at a constant c-phase flow rate. A decrease in channel width at constant flow rates not only increased the shear rate, but also enhanced the axial velocity. The increase of shear rate and axial velocity exerted a stronger viscous force on the droplet. In other words, by applying a greater change in the flow conditions, the droplet size can be controlled over a broader range.

## V. CONCLUSION

This work contributes to our understanding of the effect of channel size on droplet size in the co-flow droplet generators. This study showed that droplet size can be fine-tuned using a deformable wall. Such systems generate droplets over a broader range by changing the local flow conditions. This makes the current device suitable for the applications in which it is intended to change droplet size at a constant flow rate.

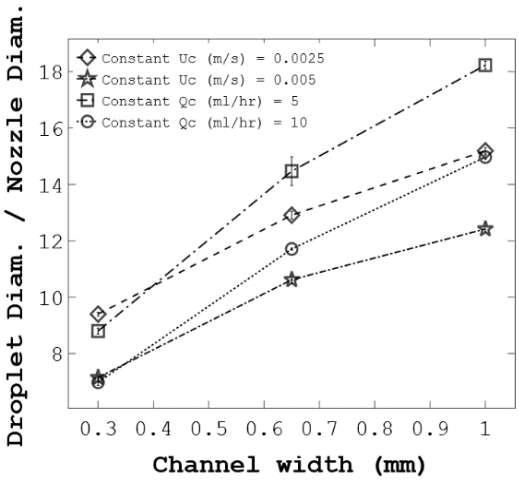


Figure 7. Effect of channel width on droplet diameter at constant c-phase velocity ($U_c$) and constant c-phase flow rate ($Q_c$). The droplet size change at a constant flow rate is more because of the increase of axial velocity.

## REFERENCES

[1] K. Keshoju and L. Sun, "Mechanical characterization of magnetic nanowire–polydimethylsiloxane composites," *J. Appl. Phys.*, vol. 105, no. 2, p. 23515, 2009.

[2] T. S. Shim, S. Kim, and S. Yang, "Elaborate design strategies toward novel microcarriers for controlled encapsulation and release," *Part. Part. Syst. Charact.*, vol. 30, no. 1, pp. 9–45, 2013.

[3] I. Polenz, Q. Brosseau, and J.-C. Baret, “Monitoring reactive microencapsulation dynamics using microfluidics,” *Soft Matter*, vol. 11, no. 15, pp. 2916–2923, 2015.
[4] S. Hattori *et al.*, “Development of microdroplet generation method for organic solvents used in chemical synthesis,” *Molecules*, vol. 25, no. 22, p. 5360, 2020.
[5] H. Norian, R. M. Field, I. Kymissis, and K. L. Shepard, “An integrated CMOS quantitative-polymerase-chain-reaction lab-on-chip for point-of-care diagnostics,” *Lab Chip*, vol. 14, no. 20, pp. 4076–4084, 2014.
[6] A. Golberg, M. L. Yarmush, and T. Konry, “Picoliter droplet microfluidic immunosorbent platform for point-of-care diagnostics of tetanus,” *Microchim. Acta*, vol. 180, no. 9–10, pp. 855–860, 2013.
[7] H. Song, D. L. Chen, and R. F. Ismagilov, “Reactions in droplets in microfluidic channels,” *Angew. chemie Int. Ed.*, vol. 45, no. 44, pp. 7336–7356, 2006.
[8] P. Rademeyer, D. Carugo, J. Y. Lee, and E. Stride, “Microfluidic system for high throughput characterisation of echogenic particles,” *Lab Chip*, vol. 15, no. 2, pp. 417–428, 2015.
[9] W. J. Duncanson, L. R. Arriaga, W. L. Ung, J. A. Kopechek, T. M. Porter, and D. A. Weitz, “Microfluidic fabrication of perfluorohexane-shelled double emulsions for controlled loading and acoustic-triggered release of hydrophilic agents,” *Langmuir*, vol. 30, no. 46, pp. 13765–13770, 2014.
[10] P. S. Sheeran, J. D. Rojas, C. Puett, J. Hjelmquist, C. B. Arena, and P. A. Dayton, “Contrast-enhanced ultrasound imaging and in vivo circulatory kinetics with low-boiling-point nanoscale phase-change perfluorocarbon agents,” *Ultrasound Med. Biol.*, vol. 41, no. 3, pp. 814–831, 2015.
[11] A. A. Maan, A. Nazir, M. K. I. Khan, R. Boom, and K. Schroën, “Microfluidic emulsification in food processing,” *J. Food Eng.*, vol. 147, pp. 1–7, 2015.
[12] H. M. Shewan and J. R. Stokes, “Review of techniques to manufacture micro-hydrogel particles for the food industry and their applications,” *J. Food Eng.*, vol. 119, no. 4, pp. 781–792, 2013.
[13] A. S. Utada, A. Fernandez-Nieves, H. A. Stone, and D. A. Weitz, “Dripping to jetting transitions in coflowing liquid streams,” *Phys. Rev. Lett.*, vol. 99, no. 9, p. 94502, 2007.
[14] A. Shams Khorrami and P. Rezai, “Oscillating dispersed-phase co-flow microfluidic droplet generation: Multi-droplet size effect,” *Biomicrofluidics*, vol. 12, no. 3, p. 34113, 2018.
[15] A. Perro, C. Nicolet, J. Angly, S. Lecommandoux, J.-F. Le Meins, and A. Colin, “Mastering a double emulsion in a simple co-flow microfluidic to generate complex polymersomes,” *Langmuir*, vol. 27, no. 14, pp. 9034–9042, 2011.
[16] P. B. Umbanhowar, V. Prasad, and D. A. Weitz, “Monodisperse emulsion generation via drop break off in a coflowing stream,” *Langmuir*, vol. 16, no. 2, pp. 347–351, 2000.
[17] R. M. Erb, D. Obrist, P. W. Chen, J. Studer, and A. R. Studart, “Predicting sizes of droplets made by microfluidic flow-induced dripping,” *Soft Matter*, vol. 7, no. 19, pp. 8757–8761, 2011.
[18] C. Deng, H. Wang, W. Huang, and S. Cheng, “Numerical and experimental study of oil-in-water (O/W) droplet formation in a co-flowing capillary device,” *Colloids Surfaces A Physicochem. Eng. Asp.*, vol. 533, pp. 1–8, 2017.
[19] H. Fox, P. Taylor, and W. Zisman, “Polyorganosiloxanes... surface active properties,” *Ind. Eng. Chem.*, vol. 39, no. 11, pp. 1401–1409, 1947.
[20] S. Vijayan and M. Hashimoto, “3D printed fittings and fluidic modules for customizable droplet generators,” *RSC Adv.*, vol. 9, no. 5, pp. 2822–2828, 2019.